

**Complex Drug Interactions of HIV Protease Inhibitors 1: Inactivation, Induction and
Inhibition of Cytochrome P450 3A by Ritonavir or Nelfinavir.**

Brian J. Kirby, Ann C. Collier, Evan D. Kharasch, Dale Whittington, Kenneth E. Thummel,
Jashvant D. Unadkat

Work originated from: Department of Pharmaceutics (BK, DW, KT and JU), Departments of
Medicine (AC), University of Washington, Seattle WA, 98195 and Department of
Anesthesiology, Washington University, St. Louis, MO 63110 (EK).

RUNNING TITLE: Ritonavir or Nelfinavir CYP3A DDI Prediction.

Please address correspondence to:

Jashvant D. Unadkat

Department of Pharmaceutics, School of Pharmacy, Box 357610

University of Washington, Seattle WA 98195-7610

Phone: 206-543-9434

Fax: 206-543-3204

Email: jash@u.washington.edu

Number of

Text pages: 27

Tables: 3

Figures: 5

References: 28

Number of Words

Abstract: 153

Introduction: 646

Discussion: 1376

Nonstandard Abbreviations:

DDI, drug-drug interaction, RTV, ritonavir; RIF, rifampin; NFV, nelfinavir; MDZ, midazolam; PI, anti-HIV Protease inhibitors; CYP, cytochrome P450; IV, intravenous; PO, oral; AUC, area under the plasma concentration-time curve; HLMS, human liver microsomes; SCHHs, sandwich cultured human hepatocytes; sWEM, supplemented Williams E media.

ABSTRACT

Conflicting drug-drug interaction (DDI) studies with the HIV protease inhibitors (PIs) suggest net induction or inhibition of intestinal or hepatic CYP3A. As part of a larger DDI study in healthy volunteers, we determined the effect of extended administration of two PIs, ritonavir (RTV) or nelfinavir (NFV), or the induction positive control rifampin, on intestinal and hepatic CYP3A activity as measured by midazolam (MDZ) disposition after 14 day treatment with the PI in either staggered (MDZ ~12 hrs after PI) or simultaneous (MDZ and PI co-administered) manner. Oral and intravenous MDZ plasma AUCs were significantly increased by RTV or NFV and were decreased by rifampin. Irrespective of method of administration, RTV decreased net intestinal and hepatic CYP3A activity whereas NFV decreased hepatic but not intestinal CYP3A activity. The magnitude of these DDIs was more accurately predicted using PI CYP3A inactivation parameters generated in sandwich cultured human hepatocytes (SCHHs) rather than human liver microsomes (HLMs).

INTRODUCTION

The clinical use of HIV protease inhibitors (PIs) is complicated by their profound drug-drug interactions (DDIs). These interactions primarily result from inactivation and inhibition of the cytochrome P450 enzymes (CYPs) CYP3A (Kumar et al.,1996; Koudriakova et al.,1998; Lillibridge et al.,1998; Ernest et al.,2005). Ritonavir (RTV) is almost exclusively used in combination with other PIs, for its ability to inactivate CYP3A and “pharmacologically boost” bioavailability of other PIs (e.g. lopinavir, saquinavir) (Zeldin and Petruschke,2004). However, PIs may produce unexpected DDIs or fail to interact with commonly used CYP3A substrate drugs when expected. For example, with acute dosing, RTV significantly decreases alprazolam (a CYP3A substrate) clearance (Greenblatt et al.,2000). Yet, paradoxically, with chronic administration, RTV has no effect on alprazolam clearance (Norvir product labeling). In addition, although PIs are thought to be eliminated primarily by CYP3A metabolism, upon chronic administration, despite CYP3A inactivation, they induce their own clearance (Hsu et al.,1997; Bardsley-Elliot and Plosker,2000). These findings have been attributed to net induction of CYP3A (Hsu et al.,1997; Bardsley-Elliot and Plosker,2000; Greenblatt et al.,2000). This is an unsatisfactory explanation based on human liver microsomes (HLMs) studies where PIs are potent inactivators of CYP3A and therefore are predicted to completely inactivate CYP3A in vivo (Koudriakova et al.,1998; Ernest et al.,2005). Moreover, such an explanation is at odds with interaction studies with other CYP3A substrates like triazolam and zolpidem (Greenblatt et al.,2000). Co-administration of these drugs results in profound interactions with PIs, even after extended administration, suggesting net inactivation of CYP3A activity. To complicate the DDI potential even further, many PIs induce other CYPs and P-glycoprotein (P-gp) in vitro in human hepatocytes (Dixit et al.,2007) and in vivo (Hughes et al.,2007) (Norvir product labeling).

The above factors make prediction of in vivo DDIs with PIs challenging from several view points. First, is there net induction or inactivation of CYP3A activity (hepatic or intestinal) when PIs are administered chronically? Second, is net induction or inactivation of CYP3A activity dependent on staggered or simultaneous administration of the PI with the CYP3A drug? Third, can such complex interactions with PIs (including inactivation, induction and inhibition) be quantitatively predicted from HLMs or sandwich cultured human hepatocytes (SCHHs)? Fourth, are other enzymes and transporters induced by PIs and can the magnitude of such induction be predicted by SCHHs experiments? Together, these complications lead to the question “Can the complex and paradoxical DDIs with the PIs be accurately predicted when multiple modes of interaction (inactivation, induction and inhibition) are accounted for and more comprehensive in vitro tools (SCHHs) are utilized?” To address this question, we conducted a series of in vivo and in vitro studies with RTV and nelfinavir (NFV) as prototypic PIs. In this paper, we have addressed the first three points listed above; subsequent papers will address the fourth point.

Briefly, we have determined if there is net induction or inhibition of intestinal and hepatic CYP3A using intravenous (IV) and oral (PO) midazolam (MDZ) as the probe substrate after multiple doses (~14 days) of RTV (400 mg bid), NFV (1250 mg bid) or the induction-positive control rifampin (600 mg qd, RIF) in the presence or absence of co-administration (staggered or simultaneous) of the PI or RIF. Then, using data on induction (Dixit et al.,2007; Fahmi et al.,2008) of CYP3A protein and mRNA expression in human hepatocytes and inactivation of CYP3A in SCHHs or HLMs, we evaluated the ability of these in vitro models to accurately predict the magnitude of the CYP3A DDIs observed in our study. Because the PIs are capable of altering CYP3A activity by multiple mechanisms (inactivation, induction and inhibition), and

each mechanism is expected to alter CYP3A activity *in vivo*, it is important to include all three mechanisms when predicting *in vivo* interactions of the PIs with CYP3A enzymes. To do so, we used a modification (Kirby and Unadkat,2010) of a comprehensive model that includes these three mechanisms (Fahmi et al.,2008).

METHODS

Subjects and Selection Criteria

All studies were approved by the University of Washington Institutional Review Board. Healthy volunteers (18-50 years) who provided written informed consent were enrolled in the study. Exclusion criteria included an abnormal EKG, fasting blood glucose of >110 mg/dl (Study 1 only), a history of cardiac, hepatic, or renal disease, drug or alcohol abuse, HIV positive, chronic use of medications other than oral contraceptives, use of nonprescription medication that may interfere with the study, pregnant or lactating, known allergies to study drugs, or had smoked within one month of the study. Subjects were asked to avoid grapefruit containing products, cruciferous vegetables or herbal nutritional supplements for three weeks prior to and throughout the study, and to avoid any acute medication, alcohol, caffeine or dietary supplements for 24 hours before and during each study session.

Study Design

This study is part of a larger study to evaluate the mechanisms of DDIs with NFV and RTV consisting of two studies detailed in Figure 1 and Table 1. The focus of this manuscript is the CYP3A mediated DDIs and therefore only addresses the effect of RTV, NFV or RIF on IV and oral MDZ. In both studies MDZ was given after ~14 day treatment with RTV, NFV or RIF. In Study 1 (staggered administration), MDZ (either oral or IV) was given ~12 hours after the last dose of RTV, NFV or RIF. In Study 2 (simultaneous administration) oral MDZ was given with a dose of RTV or NFV or 1 hour after RIF. Study 1 was conducted in two arms (RTV and RIF treatment or NFV and RIF treatment). In study 2 all subjects were treated with RTV, NFV and RIF. Order of treatment was randomized in all studies. Subjects fasted after midnight prior to each study session. In Study 1 and Study 2 (bupropion administration only) meals were held

until two hours after administration of the cocktails. In Study 2, subjects were given a light standardized breakfast before Cocktail A (in all sessions) to minimize gastrointestinal irritation by administration of RTV or NFV.

Study drugs were purchased from the following suppliers: midazolam (1 mg/ml syrup formulation, Boehringer Ingelheim, Ridgefield, CT), midazolam (1 mg/ml IV formulation, Ben Venue Labs, Bedford, OH), nelfinavir (625 mg tablets, Agouron Pharmaceuticals, La Jolla, CA), ritonavir (100 mg tablets, Abbott Labs, Abbott Park, IL) and rifampin (300 mg capsules, Sandoz, Broomfield, CO).

Chemicals and Reagents

MDZ, 1'-OH MDZ and stable labeled (D4) analogs (internal standard for MDZ and 1'-OH-MDZ analysis, IS) were purchased from Cerilliant (Round Rock, TX). Optima grade water, methanol and methyl *t*-butyl ether (MTBE) were purchased from Fisher (St. Louis, MO). All other chemicals were reagent grade or higher.

Midazolam and Metabolite Assay

Concentrations of MDZ and 1'-OH MDZ from plasma and urine (after deconjugation with β -glucuronidase, urine only) was determined via UPLC/MS/MS (Premier XE, Waters, Milford CT) after either liquid/liquid extraction (100 μ l ammonium hydroxide and 4 ml methyl-*t*-butyl ether) or precipitation with acetonitrile (2:1 v:v). Standards (calibration range of 0.1-100 ng/ml for both MDZ and 1'-OH-MDZ, IS 10 ng/ml) and quality control samples were prepared in a similar matrix and extracted or precipitated identically to the samples. Chromatographic separation was achieved on a UPLC BEH C18 2.1x 50 mm 2 micron column, 0.3 mL/min flow rate with aqueous phase (0.1% acetic acid in water) and organic phase (0.1% acetic acid in methanol) and a rapid gradient from 95% aqueous to 100% organic over 2.5 minutes, using ion collection

parameters (m/z transitions, cone voltages and collision energy) for MDZ (326.0<291.2, 42, 27), D4 MDZ (330.0<295.2, 40, 27), 1'OH MDZ (342.0<324.2, 35, 20) and D4 1'OH MDZ (346.0<328.2, 40, 22) respectively.

Inactivation of CYP3A in SCHHS and HLMs

Inactivation parameters were calculated for RTV and NFV in HLMs (n=3 livers) and SCHHS (n=4 donors). HLM experiments were performed in duplicate at 37°C, 0.25 mg/ml protein during the pre-incubation with RTV (0- 1.0 μ M, for 0, 0.5, 1 and 2 min) or NFV (0-5 μ M, for 0, 1, 2 and 5 min), then diluted 1/10 before measuring remaining CYP3A activity by 1'OH MDZ formation (20 μ M MDZ, 3 min). Pre-incubation times were optimized to ensure adequate inactivation of CYP3A while minimizing depletion of RTV or NFV. Reactions were quenched with equal volumes ice cold methanol containing IS (50 ng/ml). Depletion of RTV or NFV during pre-incubation was monitored.

Freshly isolated human hepatocytes in a 96 well plate with matrigel or duragel overlay were purchased from Cellzdirect (Durham, NC). After a 24 hour equilibration period in serum free supplemented Williams' E media (sWEM, Cellzdirect), cells were pretreated in duplicate with RTV (0-1 μ M for 0, 1, 2.5 and 5 min) or NFV (0-5 μ M for 0, 2.5, 5 and 10 min) in sWEM (\leq 1% methanol) at 37°C with 5%CO₂. Pre-incubation times were optimized to ensure adequate inactivation of CYP3A while minimizing depletion of RTV or NFV. After pretreatment, media was removed (saved for depletion analysis), cells were washed twice with phosphate buffered saline (PBS) containing 10% fetal bovine serum (FBS) followed by one wash with PBS. Then, sWEM containing midazolam (20 μ M, \leq 1% methanol) was incubated at 37°C with 5%CO₂ for 1

hour, the media was removed and quenched with equal volumes ice cold methanol containing IS (50 ng/ml).

Relative quantification of 1'-OH MDZ formation and depletion of RTV or NFV from HLMs and SCHHs experiments was performed by LC/MS using a micromass platform LCZ in positive electrospray mode with a waters 2695 HPLC and gradient elution (0.1% acetic acid in water and methanol) on an agilent XDB-C8 2.1x50 mm, 5 micron column with a phenomenex C8 guard cartridge. RTV or NFV concentrations were log average adjusted if depletion was >10% by calculating the log interpolated RTV or NFV AUC during the incubation period divided by the incubation time (log average concentration over the pre-incubation period).

Pharmacokinetic Analysis

Noncompartmental analysis of plasma concentration-time profiles of IV and PO MDZ was performed using WinNonlin Professional v 5.0 (Pharsight Corp, Mountain View, CA). Parameters estimated included area under the plasma concentration-time curve (AUC), terminal plasma half life ($t_{1/2}$) and oral or IV clearance (Dose / $AUC_{0-\infty}$). Renal clearance (Cl_r) of MDZ was estimated by the ratio of total amount of MDZ excreted in 24 hours and MDZ AUC_{0-24} . Formation clearance of 1'-OH MDZ was estimated by the ratio of the amount of 1'-OH MDZ excreted (conjugated and unconjugated) in the 24 hour urine and MDZ AUC_{0-24} . Residual MDZ from the PO administration was stripped from the IV administration profiles using the $t_{1/2}$ from IV administration and MDZ concentration prior to IV dosing. MDZ bioavailability (F) was determined by the ratio of oral and IV clearances. Hepatic bioavailability (F_H) and gastrointestinal bioavailability (F_G) were estimated assuming negligible extrahepatic metabolism after IV administration, liver blood flow of 0.0216 L/min/kg, negligible partitioning of MDZ into red blood cells, hematocrit of 0.48 and the fraction of MDZ dose absorbed $F_{Abs} = 1.0$ (Thummel

et al.,1996). The fold-change in hepatic CYP3A intrinsic clearance ($f_{Cl_{int}}^{Hep}$) upon treatment by RTV, NFV or RIF was estimated using Eq. 1 which is a rearrangement of an equation describing the predicted AUC ratio of an IV administered drug (Kirby and Unadkat,2010). In Eq. 1, $f_{m,CYP3A,Hep}$ is the fraction of hepatic clearance via CYP3A, EH is the hepatic extraction ratio of the probe drug prior to treatment, f_{hep} is the fraction of systemic clearance as a result of hepatic clearance and $RAUC_{IV}$ is the ratio of AUC of the IV administered probe drug in the presence and absence of the DDI.

$$f_{Cl_{int}}^{Hep} = 1 + \frac{1}{f_{m,CYP3A,Hep}} \left[\frac{1}{\left(\frac{1}{EH} - 1 \right) \left[\frac{1}{f_{hep}} \left[\frac{1}{RAUC_{IV}} + f_{hep} - 1 \right] - 1 \right]} - 1 \right] \quad \text{Eq. 1}$$

The fold change in intestinal intrinsic clearance ($f_{Cl_{int}}^{GI}$) was calculated using the fold change in hepatic intrinsic clearance from Eq. 1 and a rearrangement of the Fahmi et al model (Fahmi et al.,2008) (Eq. 2). In Eq. 2, $RAUC_{PO}$ is the AUC ratio of the orally administered object drug in the presence and absence of the interaction.

$$f_{Cl_{int}}^{GI} = \frac{1}{RAUC_{PO}} * \frac{1}{f_{Cl_{int}}^{Hep} \times f_{m,CYP3A,Hep} + (1 - f_{m,CYP3A,Hep})} - F_G \quad \text{Eq. 2}$$

Statistical analysis

A paired, two tailed students T-test was used to determine if treatment significantly altered the pharmacokinetics of MDZ. As pharmacokinetic parameters are typically log-

normally distributed, we also calculated the geometric mean ratio (GMR) by exponentiation of the average difference of log transformed PK parameters. If the 90% confidence interval of the GMR included 1.0, the treatment was considered to not have significantly altered the PK parameter.

Using historical data of MDZ in healthy volunteers (Wang et al.,2001; Kirby et al.,2006), we conducted an a priori power analysis using plasma AUC of MDZ as the primary outcome measure. Assuming equal variance between control and treatment groups, our analysis indicated that n=7 would provide 80% power ($\alpha < 0.05$) to discern a 54% and 41% change in oral and IV MDZ AUC respectively.

In Vitro to In Vivo Prediction

The observed AUC ratios for IV (Eq. 3) and PO (Eq. 4) MDZ were predicted using in vitro CYP3A inactivation, induction and inhibition parameters of the PIs generated in HLMs and SCHHs (Table 2) and the following two steady state models (Fahmi et al.,2008; Kirby and Unadkat,2010) :

$$\frac{AUC'_{IV}}{AUC_{IV}} = \frac{1}{f_{hep} \left(\frac{1/EH}{\left(\frac{1}{EH} - 1 \right) \left(f_{m,CYP3A,Hep} \times f_{Clint}^{Hep} + (1 - f_{m,CYP3A,Hep}) \right) + 1} \right) + (1 - f_{hep})} \quad \text{Eq. 3}$$

$$\frac{AUC'_{PO}}{AUC_{PO}} = \frac{1}{f_{Clint}^{Hep} \times f_{m,CYP3A,Hep} + (1 - f_{m,CYP3A,Hep})} * \frac{1}{f_{Clint}^{GI} \times (1 - F_G) + F_G} \quad \text{Eq. 4}$$

For simultaneous administration (Study 2), f_{Clint}^{Hep} was calculated using unbound average concentrations ($C_{ave,u}$) of RTV, NFV or RIF as the driving force for inhibition, induction and

inactivation with a 36 hour CYP3A degradation half life following Eq. 4, $f_{Cl_{int}}^{GI}$ was calculated using the predicted unbound maximum enterocyte concentration (Obach et al.,2007) and a CYP3A degradation half live of 24 hours following the Fahmi et al. model (Fahmi et al.,2008). Parameters (E_{max} and EC_{50}) describing induction of CYP3A protein or mRNA were estimated from our previously published studies in human hepatocytes (Dixit et al.,2007). Because our in vivo MDZ induction data after RIF treatment did not allow for estimation of induction of CYP3A (hepatic extraction exceeding hepatic plasma flow), induction of another CYP3A probe drug (alfentanil) after a similar RIF treatment regimen (Kharasch et al.,2004) was used as an in vitro to in vivo calibrator for CYP3A induction by estimating a scaling factor similar to the “d” value used by Fahmi et al (Fahmi et al.,2008). The factor which allowed for adequate prediction of the AUC ratio (0.38) of alfentanil after RIF treatment (assuming $f_{m,CYP3A,Hep} = 0.98$ and $EH = 0.28$ using Eq. 1) was used to scale in vivo induction of CYP3A predicted from hepatocytes (Table 2).

In Study 1, MDZ was administered ~12 hours after a dose of RIF, RTV or NFV. Therefore, the driving force concentration for estimating $f_{Cl_{int}}^{Hep}$ for CYP3A inhibition was unbound trough concentration ($C_{min,u}$), but $C_{ave,u}$ was used for inactivation and induction. Because of the staggered administration of MDZ and RTV or NFV, the estimation of $f_{Cl_{int}}^{GI}$ using Eq. 4 is not acceptable. Therefore, we assumed intestinal CYP3A was completely abolished as a result of potent inactivation, and the recovery of intestinal CYP3A was predicted based on the 24 hour degradation half-life of CYP3A (governed by enterocyte turnover) (Greenblatt et al.,2003; Culm-Merdek et al.,2006). Based on these assumptions, intestinal CYP3A activity would

recover by ~30% after 12 hours which equates to a MDZ F'_G of 0.92. Therefore, the PO MDZ AUC ratio in Study 1 was predicted using Eq. 5 in which F'_G was set at 0.92.

$$\frac{AUC_{PO}'}{AUC_{PO}} = \frac{1}{f_{Clint}^{Hep} \times f_{m,CYP3A} + (1 - f_{m,CYP3A})} * \frac{F'_G}{F_G} \quad \text{Eq. 5}$$

RESULTS

Seven subjects (healthy volunteers; Table 1) completed each arm of Study 1 (staggered administration of the PIs and MDZ) and 9 subjects (except for NFV, n=8) completed Study 2 (simultaneous administration of the PIs and MDZ).

Midazolam Pharmacokinetics

NFV and RTV significantly increased the AUC and decreased the systemic and oral clearance of IV and PO MDZ administered in a staggered or simultaneous manner (Fig. 2 and Table 3). As expected, RIF significantly increased oral and IV clearances of MDZ in both studies. IV blood clearance of MDZ after RIF treatment was increased to 2.0 L/min which exceeds hepatic blood flow (1.5 L/min), implying extra-hepatic clearance of MDZ, likely intestinal. Midazolam oral clearances and AUC geometric mean ratios (GMRs) were not statistically different between staggered (Study 1) vs. simultaneous administration (Study 2) for all three treatments (RTV, NFV or RIF). The only statistically significant difference between staggered and simultaneous administration was 1'-OH MDZ oral formation clearance (PO $Cl_{\text{formation}}$) after treatment with RTV; simultaneous showed a greater decrease than staggered. Because of the study design (Figure 1), it was possible to evaluate the bioavailability ($F_A \cdot F_G$, F_H and F) of MDZ only with staggered administration. The oral bioavailability (F) of MDZ was significantly increased by RTV and decreased by RIF. In contrast, NFV treatment did not significantly change F of MDZ, likely a result of a greatly variable effect in the intestine. Intestinal bioavailability (F_G) was significantly increased by RTV but not statistically increased by NFV. Hepatic bioavailability (F_H) was significantly increased by NFV or RTV. Consequently, RTV significantly decreased both hepatic and intestinal CYP3A activity ($f_{Cl_{\text{int}}}^{\text{Hep}}$ and $f_{Cl_{\text{int}}}^{\text{GI}}$ respectively, whereas NFV significantly decreased only hepatic CYP3A activity ($f_{Cl_{\text{int}}}^{\text{Hep}}$

) (Table 3). Because of the apparent extra-hepatic metabolism of MDZ after RIF treatment, estimates of F_H , F_G , $f_{Cl_{int}}^{Hep}$ or $f_{Cl_{int}}^{GI}$ were not possible.

CYP3A inactivation in SCHHs and HLMs

Inactivation of CYP3A by RTV or NFV in HLMs and SCHHs showed concentration and time dependency (Figure 3, Panels A-D). In contrast to HLMs, a hyperbolic plot of λ (observed inactivation rate constant) vs. inactivator concentration was not consistently observed up to concentrations of 1 μM for RTV or 5 μM for NFV in SCHHs (Figure 3, Panels E and F respectively). Therefore, the average slope of the linear portion of this curve was determined (0.174 ± 0.037 and $0.038 \pm 0.026 \mu\text{M}^{-1}\text{min}^{-1}$ for RTV and NFV respectively). The average slopes of λ vs. inactivator concentration in SCHHs are 13- and 3.7-fold lower (RTV and NFV respectively) compared to the initial slopes (k_{inact}/K_I) in HLMs (Table 2). The individual and average slopes in SCHHs (n=4) for RTV and NFV up to 1 μM were compared to the average hyperbolic profiles in HLMs (Figure 3 Panels G and H). Using the slope of λ vs. inactivator concentration for in vivo prediction is applicable since the unbound average RTV or NFV plasma concentrations are within the linear region of the plots (<1 μM).

In Vitro to In Vivo Prediction

The in vitro to in vivo scaling factor for induction of CYP3A estimated from the RIF interaction with alfentanil (Kharasch et al.,2004) was 9.6 and 5.5 using protein and mRNA expression respectively. The predicted AUC ratios for the DDIs between MDZ and RTV, or NFV using HLMs or SCHHs derived inactivation parameters and protein or mRNA expression for induction were compared with those observed (Figure 4, Panel A). In general the HLM inactivation parameters over-predicted the interactions (above the 90%CI) irrespective of

whether CYP3A protein or mRNA data were used for induction. In contrast, the SCHHs inactivation parameters more accurately predicted the MDZ AUC ratios when either CYP3A protein or mRNA expression data were used for induction. The difference between HLM and SCHH derived inactivation parameters was also apparent when evaluating the predictability of the fold change in hepatic CYP3A activity as a result of RTV or NFV treatment (Figure 4, Panel B). When protein expression was used to predict induction, in conjunction with the SCHH derived inactivation parameters, the effect of RTV or NFV was accurately predicted. In contrast, when CYP3A4 mRNA expression was used for induction in conjunction with SCHH derived inactivation parameters, the effect of RTV on hepatic CYP3A was over-predicted (a greater decrease in hepatic CYP3A than observed), but the effect of NFV was adequately predicted.

Figure 4 Panel C validates our assumption that intestinal CYP3A activity can be predicted assuming complete inactivation of CYP3A activity after RTV or NFV dosing and estimating the intestinal recovery based on enterocyte half-life.

DISCUSSION

Because of the unpredictable nature of CYP3A-mediated DDIs with the PIs, we conducted two studies to investigate the effect of RTV and NFV on intestinal and hepatic CYP3A activity in healthy volunteers. One study was designed to measure only the net effect of inactivation and induction of CYP3A and deliberately avoid acute inhibition of CYP3A produced by concomitant administration of the PIs and MDZ whereas the second study was designed to evaluate the net effect, including inhibition of CYP3A. As a result of this study design we were able to determine if net induction of CYP3A could occur in the liver or the intestine, which has been alluded to as an explanation for paradoxical DDIs with the PIs.

As we hypothesized, chronic administration of RTV did not result in net induction of intestinal or hepatic CYP3A activity. In fact, RTV treatment decreased intestinal CYP3A activity by ~78% ($f_{Cl_{int}}^{GI} = 0.22$, 90%CI of 0.10-0.48, Table 3), consistent with that expected based on normal intestinal enzyme recovery over the 12 hour dosing interval. RTV is known to activate PXR thereby inducing transcription of CYP3A and other genes (Gupta et al.,2008). If synthesis of CYP3A was induced as little as 3-fold, recovery of ~90% of baseline CYP3A activity would be expected ($f_{Cl_{int}}^{GI}$ of 0.9). This implies that either intestinal induction is minimal to nonexistent or systemic exposure of RTV is capable of inactivating intestinal CYP3A. The effect of NFV on $f_{Cl_{int}}^{GI}$ was more variable than RTV; 2 of the 7 subjects showed no decrease, or a net increase in $f_{Cl_{int}}^{GI}$ with a GMR of 0.55 (90%CI of 0.07-6.8, not statistically significant). In contrast to RTV, the average recovery of CYP3A activity is slightly greater than expected based on intestinal enterocyte recovery half-life and time after NFV dosing, though this average is heavily influenced by two subjects showing no change or an increase in intestinal CYP3A.

NFV, like RTV is also known to activate PXR and induce CYP3A transcription (Gupta et al.,2008). This implies that either inactivation of CYP3A in the intestine may be incomplete or there is moderate and variable induction of intestinal CYP3A by NFV. The two subjects who showed no decrease or a net increase in intestinal CYP3A appear to have had adequate systemic exposure of NFV ($f_{Cl_{int}}^{Hep} = 0.27$ and 0.33) implying compliance with NFV dosing. Therefore, we speculate that these two subjects may have either had much greater intestinal induction or lower exposure of the intestinal enterocytes by systemic NFV or during the absorption process.

Staggered administration of RTV or NFV substantially decreased $f_{Cl_{int}}^{Hep}$ in a less variable way than $f_{Cl_{int}}^{GI}$ with GMRs of 0.10 (90%CI of 0.06-0.17) and 0.21 (90%CI of 0.13-0.34) respectively, (Table 3). Because MDZ was not administered IV in the simultaneous administration study it was not possible to determine if simultaneous administration of RTV or NFV resulted in a greater degree of hepatic or intestinal CYP3A inhibition. 1'-OH MDZ formation clearance was affected to a greater extent by simultaneous administration of both NFV and RTV. This implies that the DDI is not mediated solely by CYP3A inactivation, but that there is a small contribution of reversible inhibition of CYP3A in the intestine and/or liver. This difference between staggered and simultaneous administration was not observed in oral clearance which is likely due to the fact that $f_{m,CYP3A}$ is less than 1.0 making formation clearance a more sensitive measure of CYP3A activity.

In order to quantitatively predict DDIs with RTV or NFV, all three mechanisms of their interaction with CYP3A (inactivation, inhibition and induction) must be included in the predictive model. We used RIF as an in vitro to in vivo calibrator to quantitatively predict the in vivo fold-induction of CYP3A activity by the PIs based on human hepatocyte studies utilizing

protein and mRNA expression. This correction factor was 9.6 and 5.5 implying that induction of CYP3A observed in vivo is ~6-10-fold higher than that observed in hepatocytes. There are many possible reasons for this in vitro to in vivo discrepancy including insensitivity of hepatocytes to induction compared to in vivo and different in vitro versus in vivo exposure profiles to the PIs. These and other in vitro to in vivo extrapolation issues have begun to be addressed (Ripp et al.,2006; Fahmi et al.,2008; Almond et al.,2009; Fahmi et al.,2009) and will be addressed further in our next manuscript. Using RTV and NFV in vitro inhibition and inactivation parameters of CYP3A measured in HLMs, we over predicted our observed MDZ AUC ratios. This implies that in vitro HLM data predict more potent net inhibition of CYP3A activity than is observed in vivo. Therefore, we asked if SCHHs would better predict CYP3A inactivation in vivo with the PIs. Indeed, we found that inactivation of CYP3A in SCHHs is 13- and 4-fold lower for RTV and NFV respectively compared to HLMs. These differences may be even greater as a result of correcting for unbound fraction in HLMs ($f_{u,mic}$), which could be as high as 0.5 for RTV (Tran et al.,2002). Moreover, the SCHHs derived inactivation parameters more accurately predicted the observed DDIs with MDZ (Figure 4). The mechanistic basis for the difference in CYP3A inactivation between HLMs and SCHHs is unknown but we speculate that it may include canalicular efflux of RTV or NFV, intracellular metabolic depletion of the PIs or other “protective” metabolic pathways present in SCHHs that are not present in HLMs. Such processes could lower the intracellular to extracellular concentration of the PI, or the exposure of CYP3A to the inactivating species, and thus decrease the inactivation potency of the PIs. The differing magnitude of CYP3A inactivation between HLMs and SCHHs is drug specific suggesting that it is not purely a system difference, but is dependent on the inactivator tested. This may be a result of varying contribution of the three points listed above for each inactivator.

These observations are consistent with those of Zhao et al. who showed differing inactivation potency (TDI IC_{50}) between HLMs and suspended human hepatocytes for amprenavir and erythromycin but not for diltiazem, raloxifene or troleandomycin (Zhao,2008). This highlights the importance of using SCHHs to determine CYP3A inactivation as this model includes the cannalicular efflux processes that may determine intracellular drug concentrations. Historically, HLMs have provided adequate prediction of in vivo DDIs for many drugs, but as highlighted here with the PIs, RTV and NFV, this simplified system (HLMs) does not always mimic the complex system of the in vivo hepatocyte, and a more comprehensive in vitro model (SCHHs) could provide a better predictive tool of the in vivo situation. These results suggest the importance of determining the mechanistic basis for the difference in potency of inactivation between HLMs and SCHHs. Such studies could provide guidelines as to when it is necessary to use SCHHs vs. HLMs for accurate in vivo predictions of DDIs.

In summary, we have shown that multiple dose treatment of RTV results in a net decrease in hepatic and intestinal CYP3A activity irrespective of simultaneous or staggered RTV administration with the CYP3A victim drug. Thus, some other unknown mechanism(s) must be at play in the paradoxical DDIs with RTV such as alprazolam and autoinduction of the PIs. In addition, we have shown that CYP3A DDIs by the PIs are better predicted if inactivation parameters are derived from SCHHs. Our results also have clinical ramifications. In this study we used a higher dose of RTV (400 mg vs. 100 mg) for two reasons. First, this study was begun when this higher dose was more widely utilized and second, some of the paradoxical DDIs and autoinduction were observed at this higher dose. Nevertheless, our results are also applicable at the lower dose of 100 mg. Others have shown profound increases in the AUC of MDZ (28-fold) (Greenblatt et al.,2009) and triazolam (40-fold) (Culm-Merdek et al.,2006) after short term

treatment (2 days) and 20-fold increase in triazolam AUC after extended treatment (10 days) with low dose RTV (100 mg bid). Therefore, we predict that RTV, even at the lower dose (100 mg bid, Figure 5), will result in net inactivation of hepatic CYP3A activity irrespective of whether it is administered simultaneously or staggered with a CYP3A victim drug. The use of dynamic or PBPK models may provide further insight into the intestinal and hepatic first pass contribution to this prediction.

ACKNOWLEDGEMENTS

We wish to thank Eric Helgeson and Christine Hoffer for clinical study coordination.

AUTHORSHIP CONTRIBUTIONS

Participated in research design: Collier, Kharasch, Kirby, Thummel and Unadkat

Conducted experiments: Kirby and Whittington

Contributed new reagents or analytical tools: Whittington

Performed data analysis: Kirby and Whittington

Wrote or contributed to the writing of the manuscript: Collier, Kharasch, Kirby, Thummel, Unadkat and Whittington

Other: Collier and Kharasch oversaw and coordinated the conduct of the clinical studies.

REFERENCES

- Almond LM, Yang J, Jamei M, Tucker GT, and Rostami-Hodjegan A (2009) Towards a quantitative framework for the prediction of DDIs arising from cytochrome P450 induction. *Curr Drug Metab* **10**: 420-432.
- Bardsley-Elliot A and Plosker GL (2000) Nelfinavir: an update on its use in HIV infection. *Drugs* **59**: 581-620.
- Culm-Merdek KE, von Moltke LL, Gan L, Horan KA, Reynolds R, Harmatz JS, Court MH, and Greenblatt DJ (2006) Effect of extended exposure to grapefruit juice on cytochrome P450 3A activity in humans: comparison with ritonavir. *Clin. Pharmacol. Ther.* **79**: 243-254.
- Dixit V, Hariparsad N, Li F, Desai P, Thummel KE, and Unadkat JD (2007) Cytochrome P450 enzymes and transporters induced by anti-human immunodeficiency virus protease inhibitors in human hepatocytes: implications for predicting clinical drug interactions. *Drug Metab. Dispos.* **35**: 1853-1859.
- Ernest CS, 2nd, Hall SD, and Jones DR (2005) Mechanism-based inactivation of CYP3A by HIV protease inhibitors. *J. Pharmacol. Exp. Ther.* **312**: 583-591.
- Fahmi OA, Boldt S, Kish M, Obach RS, and Tremaine LM (2008) Prediction of drug-drug interactions from in vitro induction data: application of the relative induction score approach using cryopreserved human hepatocytes. *Drug Metab Dispos* **36**: 1971-1974.
- Fahmi OA, Hurst S, Plowchalk D, Cook J, Guo F, Youdim K, Dickins M, Phipps A, Darekar A, Hyland R, and Obach RS (2009) Comparison of different algorithms for predicting clinical drug-drug interactions, based on the use of CYP3A4 in vitro data: predictions of compounds as precipitants of interaction. *Drug Metab Dispos* **37**: 1658-1666.
- Fahmi OA, Maurer TS, Kish M, Cardenas E, Boldt S, and Nettleton D (2008) A combined model for predicting CYP3A4 clinical net drug-drug interaction based on CYP3A4 inhibition, inactivation, and induction determined in vitro. *Drug Metab Dispos* **36**: 1698-1708.
- Greenblatt DJ, Peters DE, Oleson LE, Harmatz JS, MacNab MW, Berkowitz N, Zinny MA, and Court MH (2009) Inhibition of oral midazolam clearance by boosting doses of ritonavir, and by 4,4-dimethyl-benziso-(2H)-selenazine (ALT-2074), an experimental catalytic mimic of glutathione oxidase. *Br. J. Clin. Pharmacol.* **68**: 920-927.

- Greenblatt DJ, von Moltke LL, Harmatz JS, Chen G, Weemhoff JL, Jen C, Kelley CJ, LeDuc BW, and Zinny MA (2003) Time course of recovery of cytochrome p450 3A function after single doses of grapefruit juice. *Clin. Pharmacol. Ther.* **74**: 121-129.
- Greenblatt DJ, von Moltke LL, Harmatz JS, Durol AL, Daily JP, Graf JA, Mertzanis P, Hoffman JL, and Shader RI (2000) Alprazolam-ritonavir interaction: implications for product labeling. *Clin. Pharmacol. Ther.* **67**: 335-341.
- Greenblatt DJ, von Moltke LL, Harmatz JS, Durol AL, Daily JP, Graf JA, Mertzanis P, Hoffman JL, and Shader RI (2000) Differential impairment of triazolam and zolpidem clearance by ritonavir. *J. Acquir. Immune Defic. Syndr.* **24**: 129-136.
- Gupta A, Mugundu GM, Desai PB, Thummel KE, and Unadkat JD (2008) Intestinal human colon adenocarcinoma cell line LS180 is an excellent model to study pregnane X receptor, but not constitutive androstane receptor, mediated CYP3A4 and multidrug resistance transporter 1 induction: studies with anti-human immunodeficiency virus protease inhibitors. *Drug Metab Dispos* **36**: 1172-1180.
- Hsu A, Granneman GR, Witt G, Locke C, Denissen J, Molla A, Valdes J, Smith J, Erdman K, Lyons N, Niu P, Decourt JP, Fourtillan JB, Girault J, and Leonard JM (1997) Multiple-dose pharmacokinetics of ritonavir in human immunodeficiency virus-infected subjects. *Antimicrob. Agents Chemother.* **41**: 898-905.
- Hughes CA, Freitas A, and Miedzinski LJ (2007) Interaction between lopinavir/ritonavir and warfarin. *CMAJ* **177**: 357-359.
- Kharasch ED, Walker A, Hoffer C, and Sheffels P (2004) Intravenous and oral alfentanil as in vivo probes for hepatic and first-pass cytochrome P450 3A activity: noninvasive assessment by use of pupillary miosis. *Clin Pharmacol Ther* **76**: 452-466.
- Kirby B, Kharasch ED, Thummel KT, Narang VS, Hoffer CJ, and Unadkat JD (2006) Simultaneous measurement of in vivo P-glycoprotein and cytochrome P450 3A activities. *J. Clin. Pharmacol.* **46**: 1313-1319.
- Kirby BJ and Unadkat JD (2010) Impact of ignoring extraction ratio when predicting drug-drug interactions, fraction metabolized, and intestinal first-pass contribution. *Drug Metab Dispos* **38**: 1926-1933.
- Koudriakova T, Iatsimirskaia E, Utkin I, Gangl E, Vouros P, Storozhuk E, Orza D, Marinina J, and Gerber N (1998) Metabolism of the human immunodeficiency virus protease inhibitors indinavir and ritonavir by human

- intestinal microsomes and expressed cytochrome P4503A4/3A5: mechanism-based inactivation of cytochrome P4503A by ritonavir. *Drug Metab. Dispos.* **26**: 552-561.
- Kumar GN, Rodrigues AD, Buko AM, and Denissen JF (1996) Cytochrome P450-mediated metabolism of the HIV-1 protease inhibitor ritonavir (ABT-538) in human liver microsomes. *J. Pharmacol. Exp. Ther.* **277**: 423-431.
- Lillibridge JH, Liang BH, Kerr BM, Webber S, Quart B, Shetty BV, and Lee CA (1998) Characterization of the selectivity and mechanism of human cytochrome P450 inhibition by the human immunodeficiency virus-protease inhibitor nelfinavir mesylate. *Drug Metab. Dispos.* **26**: 609-616.
- Obach RS, Walsky RL, and Venkatakrishnan K (2007) Mechanism-based inactivation of human cytochrome p450 enzymes and the prediction of drug-drug interactions. *Drug Metab. Dispos.* **35**: 246-255.
- Ripp SL, Mills JB, Fahmi OA, Trevena KA, Liras JL, Maurer TS, and de Morais SM (2006) Use of immortalized human hepatocytes to predict the magnitude of clinical drug-drug interactions caused by CYP3A4 induction. *Drug Metab Dispos* **34**: 1742-1748.
- Thummel KE, O'Shea D, Paine MF, Shen DD, Kunze KL, Perkins JD, and Wilkinson GR (1996) Oral first-pass elimination of midazolam involves both gastrointestinal and hepatic CYP3A-mediated metabolism. *Clin Pharmacol Ther* **59**: 491-502.
- Tran TH, Von Moltke LL, Venkatakrishnan K, Granda BW, Gibbs MA, Obach RS, Harmatz JS, and Greenblatt DJ (2002) Microsomal protein concentration modifies the apparent inhibitory potency of CYP3A inhibitors. *Drug Metab Dispos* **30**: 1441-1445.
- Wang Z, Gorski JC, Hamman MA, Huang SM, Lesko LJ, and Hall SD (2001) The effects of St John's wort (*Hypericum perforatum*) on human cytochrome P450 activity. *Clin. Pharmacol. Ther.* **70**: 317-326.
- Zeldin RK and Petruschke RA (2004) Pharmacological and therapeutic properties of ritonavir-boosted protease inhibitor therapy in HIV-infected patients. *J Antimicrob Chemother* **53**: 4-9.
- Zhao P (2008) The use of hepatocytes in evaluating time-dependent inactivation of P450 in vivo. *Expert Opin. Drug Metab. Toxicol.* **4**: 151-164.

FOOTNOTES

This work was supported by the National Institutes of Health [Grants GM032165, K24DA00417, R01DA14211]. A portion of this work was conducted through the Clinical Research Center Facility at the University of Washington and supported by the National Institutes of Health [Grant M01-RR-00037]. Brian Kirby was supported in part by an ARCS fellowship, a National Institutes of Health Pharmacological Sciences training grant [Grant GM07550] and a Simcyp sponsored fellowship.

FIGURE LEGENDS

Figure 1: Study design showing administration of probe drug cocktails prior to and after RTV, NFV or RIF treatment. In Study 1, the probe drug cocktails were staggered ~12 hours after the last dose of RTV, NFV or RIF. In Study 2, a dose of RTV, NFV or RIF was simultaneously administered with MDZ. For details on the components of cocktails, see Table 1.

Figure 2: Mean (\pm SD) plasma concentration-time profiles of oral (A) and IV (B) MDZ prior to (CON) or after treatment with RTV, NFV or RIF. In Study 1 (dashed lines and open symbols) MDZ administration was staggered ~12 hrs after the last dose of RTV, NFV or RIF whereas in Study 2 (solid lines and closed symbols) MDZ was simultaneously administered with a dose of RTV, NFV or RIF.

Figure 3: CYP3a inactivation by RTV or NFV in HLMs versus SCHHs. Natural log percent remaining CYP3A activity after RTV (A, C) or NFV (B, D) pretreatment measured in representative HLMs and SCHHs lots (μ M concentrations of the inactivator are listed on the right of each panel). A combined plot of observed inactivation rate (λ , min^{-1}) of CYP3A by RTV (E) or NFV (F) in representative HLMs and SCHHs lots. A combined plot of the linear fit of λ (min^{-1}) of CYP3A by RTV (G) or NFV (H) in four different SCHHs (grey lines) and average linear fit (dashed line) compared to the average hyperbolic plot measured in HLMs (n=3).

Figure 4: The observed (GMR \pm 90%CI) MDZ AUC ratios (A) (black bars with error bars) or fold change in hepatic CYP3A activity (B) caused by RTV or NFV were more accurately predicted using CYP3A4 mRNA expression (circles) or CYP3A protein (squares) for induction with inactivation parameters of CYP3A by RTV or NFV derived from SCHHs (closed symbols) compared to HLMs (open symbols). Observed (GMR \pm 90%CI) intestinal CYP3A recovery (black bars with error bars) was accurately predicted by intestinal CYP3A recovery based on intestinal turnover (C).

Figure 5: The predicted contribution of inhibition, inactivation and induction of hepatic CYP3A by RTV is shown across an applicable RTV total plasma concentration range indicating that even at low dose RTV (100 mg bid, \sim 1 μ M) net hepatic CYP3A inactivation is predicted.

Table 1: Subject Characteristics and Treatment Period Length

Subject Characteristics			
		Study 1 Staggered	Study 2 Simultaneous
Race	Caucasian (non-hispanic/latino)	14	9
	Asian	1	0
	Black/African American	1	0
Gender	Male	5	3
	Female	11	6
Age (yrs)	Mean \pm SD	33 \pm 9	29 \pm 9
	Range	20 – 50	18 - 42
Weight (kg)	Mean \pm SD	78 \pm 14	79 \pm 14
	Range	60 - 100	59 - 105
Treatment Period in Days: Average (min,max)			
		Study 1 Staggered	Study 2 Simultaneous
	Ritonavir (200 mg tid day 1, 300 mg bid days 2-7, 400 mg bid \geq day 8, dose escalation to minimize GI irritation)	14 (14,15)	15 (15,15)
	Nelfinavir (1250 mg bid)	14 (13,16)	14 (14,15)
	Rifampin (600 mg qd)	14 (12,15)	15 (14,15)
Probe Drug Administration			
Cocktail A	2 mg PO midazolam @~8am, 0.5 mg PO digoxin @~9am (24 hour blood and urine collection)		
Cocktail B	1 mg IV midazolam, 30 mg PO dextromethorphan, 500 mg PO tolbutamide, 200 mg PO caffeine @~8am. (24 hour blood and urine collection)		
Bupropion	150 mg PO extended release bupropion @~8am. (48 hr blood and urine collection)		

Table 2: Parameters Used for Midazolam AUC Ratio Predictions

Midazolam Parameters													
EH		f_{Hep}		$f_{\text{m,CYP3A,Hep}}$		F_G		F_G' (Study 1 Staggered)					
0.57		0.994		0.92		0.78		0.92					
Precipitant Parameters													
				CYP3A Inhibition		CYP3A Inactivation				CYP3A Induction (protein) [#]			
						HLMs (n=3)*		SCHHs (n=4)*	HLMs/SCHHs slope	Protein [#]		mRNA Expression [#]	
	Dose	C_{ave} (μM)	f_u	$K_{i,\text{CYP3A}}$ (μM)	K_i (μM)	k_{inact} (min^{-1})	$k_{\text{inact}}/K_i^{\dagger}$ ($\mu\text{M}^{-1}\text{min}^{-1}$)	Slope ($\mu\text{M}^{-1}\text{min}^{-1}$)		$EC_{50,\text{CYP3A}}$ (μM)	E_{max} (fold)	$EC_{50,\text{CYP3A}}$ (μM)	E_{max} (fold)
RTV	400 mg bid	8	0.015	0.25	0.25 (102%)	0.33 (21%)	2.31 (71%)	0.174 (22%)	13.3	3.4	13.9	23.8	67.9
NFV	1250 mg bid	4	0.015	1.8	1.82 (70%)	0.16 (36%)	0.14 (80%)	0.038 (67%)	3.7	6.5	11.2	3.4	17.2
RIF	600 mg qd	2	0.2	18.5	N/A					9.7	21.9	16.3	62.6

*Average values (%CV), [#]Estimated from Dixit et al. 2007, f_u unbound fraction in plasma, $K_{i,\text{CYP3A}}$ reversible CYP3A inhibition constant, $EC_{50,\text{CYP3A}}$ Concentration that results in half maximum CYP3A protein or mRNA induction, E_{max} maximum fold induction of CYP3A protein or mRNA, [†] reported value is the average (%CV) of k_{inact}/K_i estimated for each HLM.

Table 3: MDZ Pharmacokinetic Parameters Before and After Treatment with NFV, RTV or RIF

	Control	Nelfinavir		Ritonavir		Rifampin		
		Ave ± SD	GMR (90% CI)	Ave ± SD	GMR (90% CI)	Ave ± SD	GMR (90% CI)	
Study 2 midazolam simultaneously administered with NFV, RTV or RIF								
PO	AUC _{0-∞} (hr*ng/ml)	25.7 ± 10.4	136 ± 33	5.8 (4.5-7.5)	266 ± 99	10.5 (8.7-12.7)	2.49 ± 0.74	0.10 (0.08-0.13)
	Cl _{oral} (L/min)	1.51 ± 0.6	0.26 ± 0.05	0.17 (0.13-0.22)	0.14 ± 0.05	0.10 (0.08-0.12)	14.5 ± 4.1	10.0 (7.7-12.9)
	Cl _{oral} (ml/min/kg)	19.5 ± 8.3	3.36 ± 0.86	0.17 (0.13-0.22)	1.85 ± 0.70	0.10 (0.08-0.12)	185 ± 51.3	10.0 (7.7-12.9)
	Cl _{formation} (L/min)	1.10 ± 0.5	0.12 ± 0.04	0.11 (0.08-0.15)	0.05 ± 0.02	0.05 (0.04-0.06)	9.2 ± 2.9	8.8 (6.7-11.4)
	T _{1/2} (hr)	4.7 ± 1.8	5.5 ± 2.5	1.2 (1.03-1.5)	14 ± 7.7	2.9 (2.5-3.4)	1.5 ± 0.6	0.33 (0.27-0.41)
Study 1 midazolam staggered administered with NFV, RTV or RIF								
PO	AUC _{0-∞} (hr*ng/ml)	22.7 ± 9.4	77.4 ± 51.5	3.3 (1.9-5.5)	188 ± 33.0	8.4 (6.8-10.4)	1.84 ± 0.67	0.09 (0.07-0.11)
	Cl _{oral} (L/min)	1.73 ± 0.7	0.62 ± 0.38	0.31 (0.18-0.52)	0.18 ± 0.04	0.12 (0.10-0.15)	20.3 ± 7.1	11.7 (9.3-14.8)
	Cl _{oral} (ml/min/kg)	24.7 ± 11.5	8.41 ± 6.44	0.31 (0.18-0.52)	2.43 ± 0.55	0.12 (0.10-0.15)	265 ± 94.4	11.7 (9.3-14.8)
	Cl _{formation} (L/min)	1.14 ± 0.5	0.40 ± 0.27	0.27 (0.15-0.50)	0.10 ± 0.05	0.10 (0.07-0.14)	9.8 ± 3.8	8.3 (6.4-10.8)
	T _{1/2} (hr)	3.8 ± 1.5	4.4 ± 1.5	1.1 (0.90-1.4)	11.4 ± 3.8	3.2 (2.6-3.9)	0.97 ± 0.30	0.27 (0.22-0.32)
IV	AUC _{0-∞} (hr*ng/ml)	36.2 ± 10.4	66.3 ± 22.0	2.0 (1.7-2.4)	120 ± 23.6	3.0 (2.7-3.4)	16.1 ± 2.9	0.48 (0.43-0.54)
	Cl _{IV} (L/min)	0.49 ± 0.11	0.28 ± 0.09	0.51 (0.42-0.61)	0.14 ± 0.03	0.33 (0.30-0.37)	1.06 ± 0.17	2.1 (1.8-2.3)
	Cl _{IV} (ml/min/kg)	6.68 ± 1.62	3.51 ± 1.17	0.51 (0.42-0.61)	1.92 ± 0.56	0.33 (0.30-0.37)	13.9 ± 2.32	2.1 (1.8-2.3)
	Cl _{formation} (L/min)	0.34 ± 0.08	0.16 ± 0.08	0.41 (0.29-0.56)	0.05 ± 0.02	0.19 (0.16-0.22)	0.68 ± 0.10	1.9 (1.7-2.1)
	T _{1/2} (hr)	4.1 ± 1.5	5.8 ± 4.2	1.2 (0.89-1.7)	11.7 ± 6.3	2.7 (2.5-3.0)	2.5 ± 1.1	0.65 (0.57-0.73)
F	0.31 ± 0.09	0.61 ± 0.24	1.7 (0.97-2.9)	0.79 ± 0.13	2.8 (2.3-3.3)	0.06 ± 0.02	N/A*	0.18 (0.15-0.23)
F _H	0.43 ± 0.15	0.69 ± 0.10	1.8 (1.5-2.1)	0.83 ± 0.05	1.8 (1.5-2.2)			
F _A *F _G	0.78 ± 0.25	0.89 ± 0.37	0.96 (0.60-1.5)	0.96 ± 0.20	1.5 (1.4-1.7)			
Hep Cl _{int} fold change ($f_{Cl_{int}}^{Hep}$)			0.24 ± 0.11	0.21 (0.13-0.34)	0.12 ± 0.09	0.10 (0.06-0.17)	N/A*	
GI Cl _{int} fold change ($f_{Cl_{int}}^{GI}$)			0.38 ± 1.4	0.55 (0.07-6.8)	-0.04 ± 0.45	0.22 (0.10-0.48)		

Bolded values are significantly different than control (p<0.05, paired T-test) or the 90% CI does not include unity. * F_H, F_A*F_G, $f_{Cl_{int}}^{GI}$ and $f_{Cl_{int}}^{Hep}$ are not available for MDZ after RIF treatment because of IV blood clearance exceeding the estimated hepatic blood flow. All reported clearance values are plasma clearances.

Downloaded from dmd.aspetjournals.org at ASPET Journals on April 19, 2024

Figure 1:

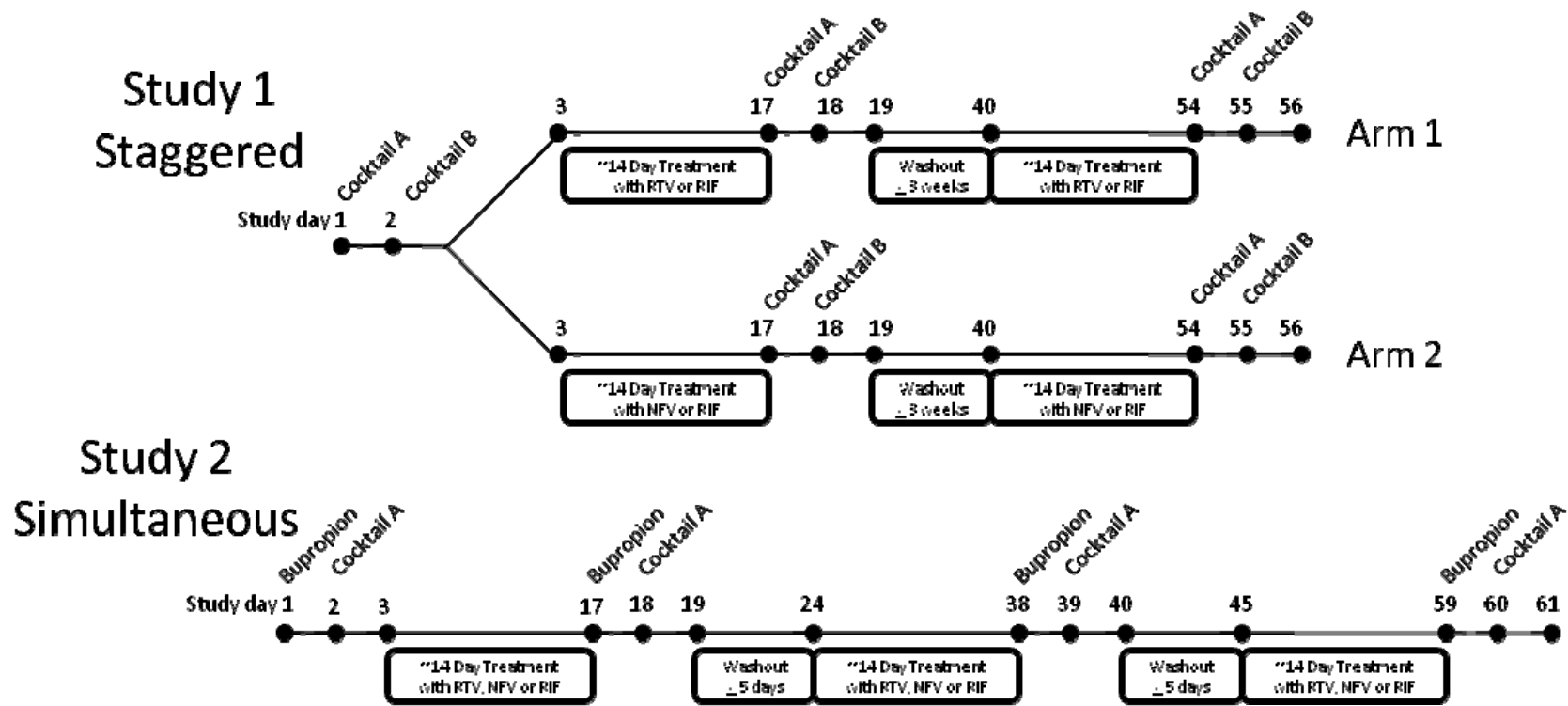
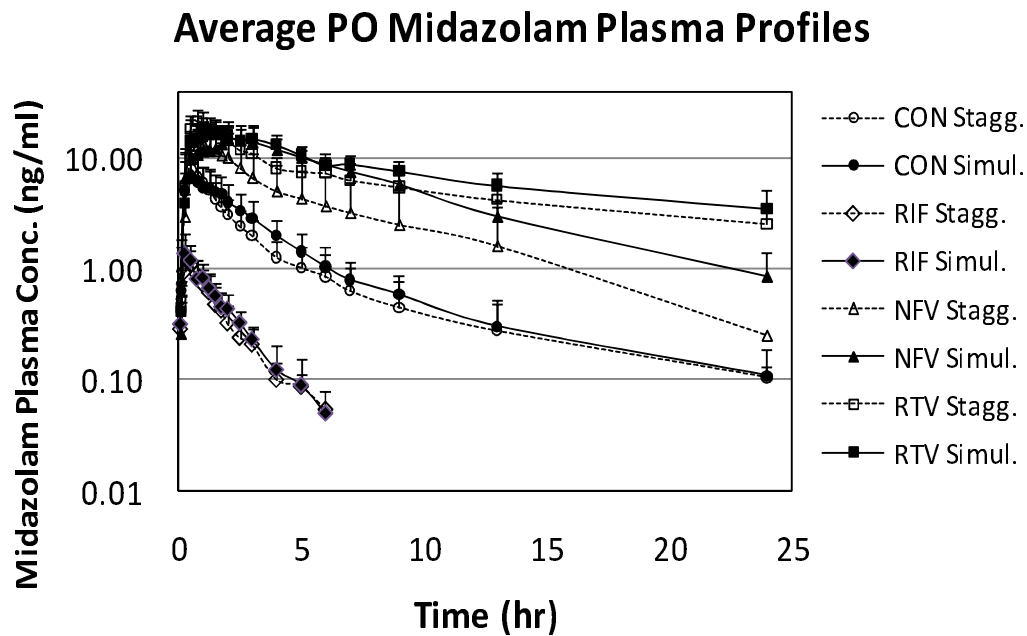


Figure 2:

A



B

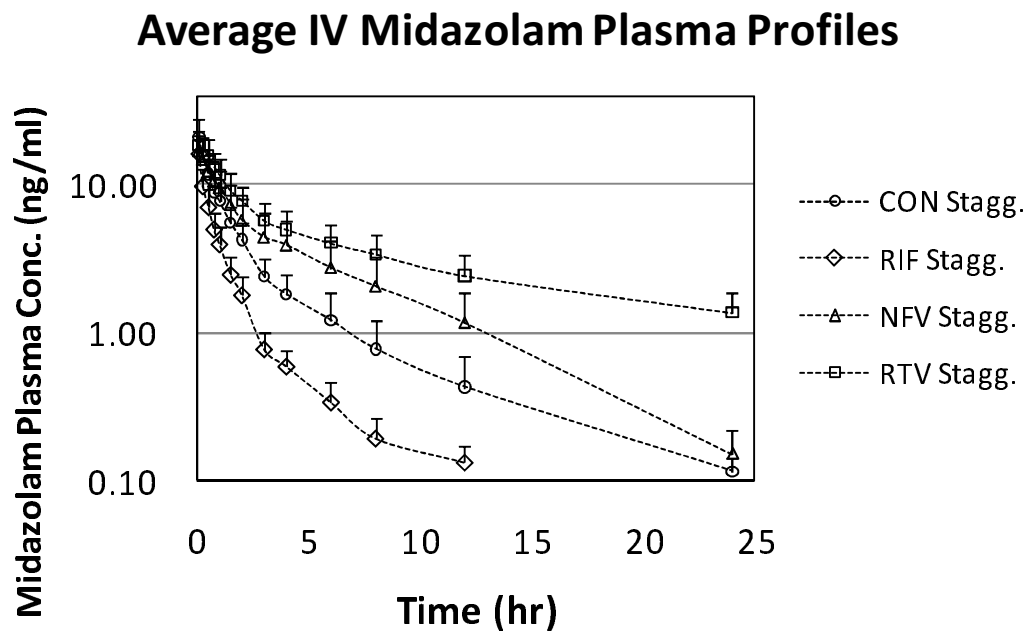


Figure 3:

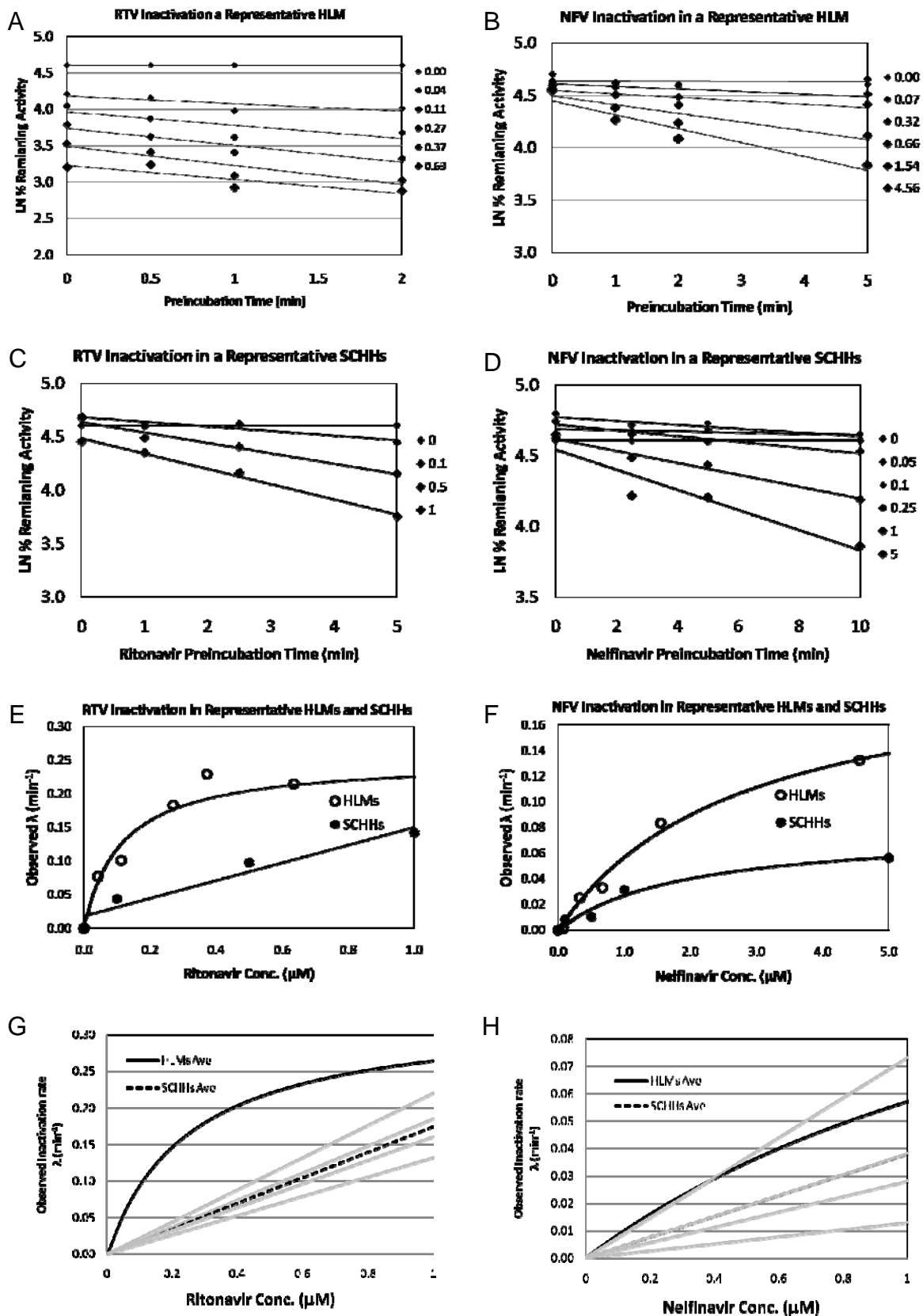


Figure 4:

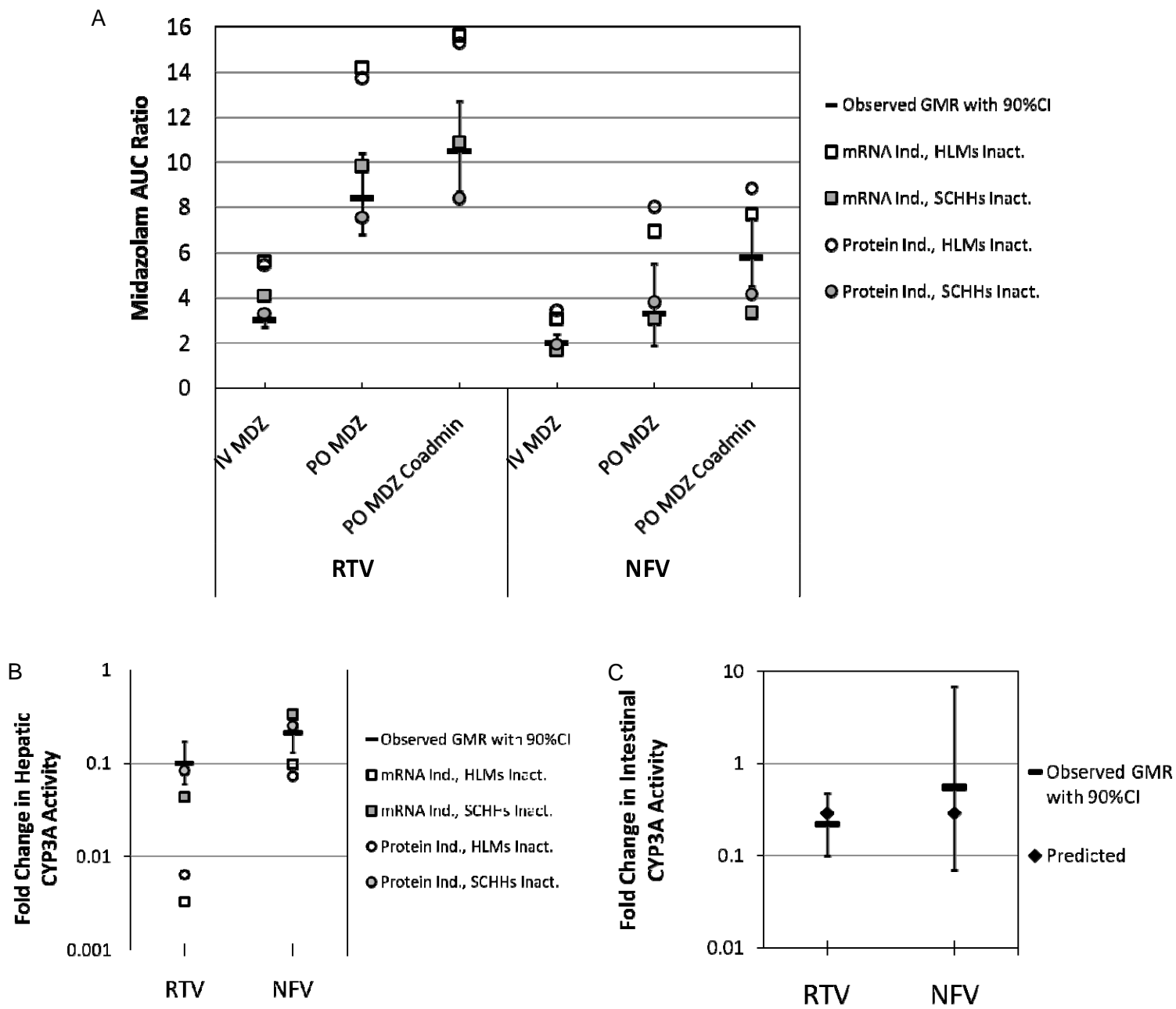


Figure 5:

